Journal of Oceanology and Limnology
Vol. 42, No. 2, pp. 594-608, 2024
https://doi.org/10.1007/s00343-023-3003-y

Research Paper

Differential expression of miRNAs and mRNAs in the livers of largemouth bass *Micropterus salmoides* under heat stress*

Xuqian ZHAO#, Zijie LIN#, Caijuan LI, Hao ZHU, Lingling LI, Wenjia MAO, Qufei LING**

School of Biology and Basic Medical Sciences, Suzhou Medical College of Soochow University, Suzhou 215000, China

Received Jan. 2, 2023; accepted in principle Mar. 22, 2023; accepted for publication May 5, 2023

© Chinese Society for Oceanology and Limnology, Science Press and Springer-Verlag GmbH Germany, part of Springer Nature 2024

Abstract Global warming threatens freshwater ecosystems and compromises fish survival. To elucidate the role of miRNAs in the livers of heat stressed largemouth bass, juvenile fish was subject to heat stress under 37 °C. Both mRNA-seq and miRNA-seq were conducted on the liver tissues under control and heat stress conditions. Differential gene expression analysis and enrichment analysis were performed on mRNA and miRNA expression profiles. A total of 406 differentially expressed genes (DEGs) were discovered, of which 212 were up-regulated and 194 were down-regulated. Most of the DEGs were significantly implicated in the regulation of "protein processing in endoplasmic reticulum", "proteasome", "steroid biosynthesis", and "ornithine decarboxylase inhibitor activity" pathways. In addition, 47 differentially expressed miRNAs (DEMs) were identified in largemouth bass livers under heat stress, including 21 up-regulated and 25 down-regulated miRNAs. A negatively regulated miRNA-mRNA network including 12 miRNAs and 19 mRNAs was constructed with DEMs involved in "protein degradation", "calcium ion regulation", "cell apoptosis", and "lipid metabolism". Moreover, this study indicated novel-miR-144 activated the IRE1 signaling pathway by targeting txndc5 to induce liver apoptosis in largemouth bass under heat stress. This study revealed the involvement of miRNA regulation in largemouth bass in response to heat stress.

Keyword: heat stress; largemouth bass; miRNA-mRNA interaction

1 INTRODUCTION

Climate change along with rising water temperature and increasing extreme temperature events is a fundamental threat to freshwater ecosystems and has concomitant effects on freshwater fish (Johnson et al., 2018; Olusanya and van Zyll de Jong, 2018; Woolway and Merchant, 2019). Freshwater fish are ectotherm, whose physiological and biochemical processes are controlled by internal body temperatures, and thus vulnerable to the high-water temperature (Alfonso et al., 2021). High water temperatures have been linked to major shifts in fish growth, reproduction, immunity, and have even led to the elimination of fish populations (Kao et al., 2020).

To mitigate the detrimental influences of heat stress, fish adaptively regulate physiological responses. For instance, red-band trout (*Oncorhynchus mykiss gairdneri*) and Chinese minnow (*Rhynchocypris oxycephalus*) showed adaptive pattern of thermal tolerance through reducing physiological costs of heat shock protein (HSP) production (Narum and Campbell, 2015; Yu et al., 2018). Barramundi (*Lates calcarifer*) increase the expression of the molecular chaperone, Hsp90a.2, to protect from heat-induced damage

* Supported by the Scientific Fund of Jiangsu Province (No. BY2015039-10), the Aquatic Three Project of Jiangsu Province (No. Y2017-37), the Priority Academic Program Development of Jiangsu Higher Education Institutions (PAPD), the Top-notch Academic Programs Project of Jiangsu Higher Education Institutions (TAPP), and the Jiangsu Funding Program for Excellent Postdoctoral Talent

** Corresponding author: lingqf@suda.edu.cn

# Xuqian ZHAO and Zijie LIN contributed equally to this work and should be regarded as co-first authors.

(Newton et al., 2013). Under heat stress, lemon damselfish (*Pomacentrus moluccensis*) increase gene expression of the protein turnover pathway, which may relieve heat-induced protein damage (Kassahn et al., 2007).

Thanks to the advance of next-generation sequencing, transcriptomic analysis of fish tissues largely improves the understanding fish physiology under heat stress. For instance, heat stress significantly affects gene expression profiles in the livers of Atlantic salmon (*Salmo salar*) and Spotted seabass (*Lateolabrax maculatus*) (Shi et al., 2019; Cai et al., 2020). Especially, MicroRNA (miRNA) is a non-coding RNA for post-transcriptional regulation through mRNA silencing or degradation (Mori et al., 2019). Moreover, miRNAs may play crucial roles in responses to environmental changes. For example, differentially expressed miRNAs (DEMs) mediated immunosuppressive injury in common carp (*Cyprinus carpio*) spleens caused by cadmium (Chen et al., 2020). Sun et al. (2020) found that miR-125 and miR-205 down-regulated CPT1 to inhibit β-oxidation in largemouth bass (*Micropterus salmoides*) livers under acute hypoxia. The liver is a crucial metabolic organ associated with stress responses, and heat stress can cause severe damage to the livers of the Chinese giant salamander (*Andrias davidianus*) and pikeperch (*Sander lucioperca*) (Wang et al., 2018, 2019). Recent study reported the miRNAs networks in kidneys of heat stressed rainbow trout (*Oncorhynchus mykiss*) (Zhou et al., 2019). Moreover, two studies found DEMs in the liver tissues of rainbow trout (*Oncorhynchus mykiss*) under heat stress, and the target genes of the DEMs were mainly related to protein homeostasis (Huang et al., 2018). The livers of heat stressed *Cyprinus carpio* showed 29 significant differential expression miRNAs, whose target genes were associated with insulin signaling and lipid metabolism (Sun et al., 2019). Those literatures suggested that miRNAs might be an important regulators of heat stress response in fish, while the generality of this consideration remains to be verified across different fish species.

Largemouth bass, a freshwater fish species, is widely distributed in lakes and reservoirs of North America. More than a gaming fish, it has been intensively cultured in China for past two decades (Bae et al., 2018; Huang et al., 2021). The optimum water temperature for largemouth bass growth ranges 26–29 °C (Díaz et al., 2007). Summer temperatures have reached or exceeded 30 °C in some lakes, and even recently peaked at 35–37 °C, which is highly challenging for largemouth bass survival (White and Wahl, 2020). Accordingly, understanding the physiology of heat stressed largemouth bass has ecological and economic benefits. Our previous study showed that heat stress induced endoplasmic reticulum stress, which further triggered apoptosis in the livers of largemouth bass (Zhao et al., 2022). To clarify the roles of miRNAs in the heat stressed largemouth bass, we controlled the thermal environment under laboratory conditions and conducted an integrated analysis of miRNAs and mRNAs profiles. Our objectives were to understand whether miRNAs participate in largemouth bass responses to heat stress and reveal the potential molecular regulation mechanism.

2 MATERIAL AND METHOD

2.1 Material

2.1.1 Fish

We bought thirty-six farmed largemouth bass (average body weight: 130±27.6 g, average body length: 20±1.4 cm, i.e., mean±S.D.) from Suzhou Jinchengfu Fishery Science and Technology Development Co., Ltd., Jiangsu Province, China. The fish were cautiously transferred to cylindrical experimental tanks (tank inner radius: 0.4 m, tank height: 0.7 m, volume of circulating aerated fresh water: 200 L, dissolved oxygen: >8 mg/L, ammonia nitrogen and nitrite: <0.24 mg/L, pH: 8±0.1) of automatic temperature-controlled recirculating systems (Shanghai Haishen Industry & Trade Co., Ltd.). During one-week acclimatization, the water temperature of the experimental tanks was kept at 27 °C, and fish were fed to visual satiety twice a day with a commercial diet containing 45% crude protein, 10% crude lipid, 16% crude ash, and 5% crude fiber provided by Xinxin Tianen Co., Ltd., Zhejiang Province, China.

2.1.2 Cultured primary hepatocyte

To study the impact of heat stress in vitro, largemouth bass primary hepatocytes were harvested using a trypsin method following the previous literature with minor modification (Xiang et al., 2021). Briefly, liver tissues were collected from five largemouth bass (body weigh 15–20 g) and minced into small pieces (about 1 mm^3) using surgical scissors. Immediately, the liver tissues were digested with 0.25% trypsin-EDTA at 28 °C for about 30 min. The digested tissues were filtered through a

100-μm mesh sieve. The obtained suspension of hepatocytes was then diluted to 1×10^6 cells/mL medium and placed into three 25-cm^2 culture flasks. The cultured cells were resuspended in M199/L-15 medium containing 15% fetal bovine serum and placed in a 4% CO_2 humidified incubator at 28 °C.

2.2 Method

2.2.1 Heat treatment and sampling

The heat stress experiment was conducted following the previous study with minor modification (Cheng et al., 2018). Specifically, after one-week acclimatization, fish were fasted for one day before the heat treatment. All specimens of largemouth bass were randomly divided into a control check group (CK, *n*=18) and a heat treatment group (HT, *n*=18). For the CK group, the water temperature was maintained at 27 °C (±0.5 ℃), which is the same as the water temperature during the acclimatization. For the HT group, the water temperature was elevated from 27 °C to 37 °C through gradual increases of 1 °C per hour and then maintained at 37 °C (±0.5 ℃) for 6 h. After the heat experiment, nine fish were collected from each of the CK and HT groups, anesthetized with 200-mg/L MS-222 (Sigma, USA), and then dissected promptly for liver sampling. Each liver was divided into three sub-samples, and immediately stored at -80 °C for Hematoxylin and Eosin (H&E) Staining, mRNA sequencing, miRNA sequencing, respectively.

2.2.2 Histopathological analysis of livers

To visually examine the histopathological differences of livers under control and heat stress condition, H&E staining was conducted. Specifically, fixed liver tissues were dehydrated in ethanol, embedded in paraffin, sectioned to a thickness of 5 μm, and stained. Then, slides were sealed with neutral balsam and observed and photographed under a microscope (Leica, DM750).

2.2.3 Library preparation and sequencing

Total RNA was extracted from liver tissues with TRIzol reagent (TaKaRa, Japan) following the manufacturer's instructions. The genomic DNA was removed with DNase I (NEB, USA). Subsequently, RNA samples with high quality (RNA integrity number >8.0 and Optical density: 260/280 >1.8) were used for preparing mRNA and miRNA sequencing libraries. Notably, RNA samples of three fish individuals were pooled together as one replicate, and this procedure was practiced for both mRNA and miRNA sequencing. For mRNA sequencing, six libraries (heat treatment group: HT1, HT2, and HT3; control check group: CK1, CK2, and CK3) were constructed with NEBNext® Ultra™ Directional RNA Library Prep Kit (NEB, USA), followed by paired-end sequencing on Illumina HiSeq 2000 platform with TruSeq PE Cluster Kit v4-cBot-HS (Illumia, USA) according to the manufacturer's instructions. For miRNA sequencing, six libraries (HT1, HT2, HT3, CK1, CK2, and CK3) were constructed with NEB Small RNA Library kit (NEB, USA), and single-end sequencing was performed on Illumina HiSeq 2000 platform with TruSeq PE Cluster Kit v4-cBot-HS (Illumia, USA) following the manufacturer's instructions. Both mRNA and miRNA sequencing were performed by Biomarker Technologies Technology Co., Ltd. (Beijing, China).

2.2.4 Pre-processing deep-sequencing data

Raw reads from next generation sequencing were pre-processed using a customized Perl script. Concretely, reads containing Illumina adapters, and low-quality reads were trimmed under the following criteria: percentage of bases with Q scores: <20; percentage of unidentified bases: >10%. The reads of miRNA libraries were further trimmed by removing sequences smaller than 18 nt or longer than 30 nt. To examine trimming quality, average of GC-content per read, average sequencing quality score (Q scores) of the clean data were calculated.

Based on the mRNA datasets, de novo transcriptome assembly was constructed using Trinity (v2.5.1) (Grabherr et al., 2011) with the following augments "*-min_contig_length 200 -group_pairs_distance 500*". Subsequently, gene function was annotated to the de novo assembly according to the following databases: NR (Non-Redundant Protein Sequence Database) (NCBI Resource Coordinators, 2018); Pfam (Mistry et al., 2021); Swiss-Prot (Bairoch and Apweiler, 1997); KEGG (Kyoto Encyclopedia of Genes and Genomes) (Kanehisa et al., 2010); GO (Gene Ontology) (Ashburner et al., 2000). After the construction and annotation of de novo transcriptome assembly, the filtered reads from mRNA sequencing were mapped on the assembly using Bowtie (v1.0.0) software (Langmead et al., 2009). RSEM (v1.2.19) software (Li and Dewey, 2011) was used to calculate the expression values for the downstream analysis. Specifically, *rsem-prepare-reference* function was used to build RSEM reference and then *rsem-*

calculate-expression function was performed to calculate the expression values.

For the miRNA datasets, Bowtie (v1.0.0) with augments "*-v 0*" was used to identify rRNA, tRNA, snRNA, snoRNA, ncRNA, and other ncRNA according to Silva (Quast et al., 2013), GtRNAdb (Chan and Lowe, 2009), Rfam (Kalvari et al., 2021), and Repbase (Bao et al., 2015) databases. To detect miRNAs, the remaining reads were mapped against the pikeperch (*Sander lucioperca*) reference genome (NCBI accession number PRJNA576669) (Nguinkal et al., 2019) and known miRNAs in miRNA (v22) database using Bowtie (v1.0.0) with augments "*-v 0*". To identify the known miRNAs and detect the novel miRNAs, quantifier. pl function in miRDeep2 (v2.0.5) (Friedländer et al., 2012) with parameters "-g -1" was used.

2.2.5 Differential gene expression analysis

To find out differentially expressed mRNAs and miRNAs, differential gene expression analysis was performed using R/DESeq2 (v1.10.1) (Love et al., 2014) software. Specifically, the read counts of mRNA and miRNA expression data were first transformed to fragments per kilo base of transcript per million mapped fragments (FPKM) and transcripts per million (TPM), respectively. Then, the transformed expression data was fit using a model based on the negative binomial distribution. Wald test was performed to calculate the *P*-values for differentially expression mRNAs and miRNAs. The obtained *P*-values were adjusted using the Benjamini and Hochberg's approach for controlling the false discovery rate. Differentially expressed mRNAs and miRNAs were identified using $|\log_2(\text{fold change})| \geq 0.58$ and adjusted $P \leq 0.05$. GO and KEGG database were referred to identify the biological functions of the differentially expressed genes (DEGs).

2.2.6 Enrichment analysis

To explore the biological function of DEGs, GO term and KEGG pathway enrichment analyses were performed using ClueGO (v2.5.7) (Bindea et al., 2009) plug-in in Cytoscape (v3.8.0) (Shannon et al., 2003). The GO terms and KEGG pathways with an adjusted $P<0.05$ were considered significant (Bonferroni step-down method).

2.2.7 Target gene prediction and miRNA-mRNA regulatory network construction

Target genes of DEMs were predicted using miRanda 3.3a (Enright et al., 2003) and TargetScan (v5.0) (McGeary et al., 2019). Only the intersections among the potential predicted target genes of DEMs and DEGs were recognized as target genes for DEMs. Based on the regulatory relationship between miRNAs and mRNA in this experiment, miRNA-mRNA regulatory networks were constructed and visualized using Cytoscape (v3.8.0).

2.2.8 Heat treatment on cultured primary hepatocytes

Following cell attachment (cell confluency= 70%–80%), the temperature in the CO_2 incubator was elevated from 28 to 37 °C (1 °C/h) and maintained at the experimental temperature for 6 h. Meanwhile, the control group was maintained at 28 °C. Total RNA from the primary hepatocytes was extracted with RNA extraction reagent (Nuoweizan Biotechnology Co., Ltd., Nanjing, China) according to the recommended instructions and stored at -80 °C.

2.2.9 Quantitative real-time PCR

To verify the accuracy of sequencing data, ten DEMs were randomly selected for quantitative real-time PCR (qRT-PCR) using a qTOWER 2.0 cycler (Jena, Germany). The specific primers of mRNAs and miRNAs (Supplementary Tables S1 & S2, respectively) used for analysis were synthesized by Shanghai Sangon Biotechnology Co., Ltd. (Shanghai, China). cDNA was synthesized from 1-μg total RNA using a miR-XTM miRNA First-Strand Synthesis Kit and PrimeScript RT Master Mix (TaKaRa, Japan). Then qRT-PCR was conducted using SYBR Green PCR Master Mix (TaKaRa, Japan). The PCR system for mRNA used 20-μL reactions with the following conditions: 95 °C for 1 min; 95 °C for 5 s, 60 °C for 30 s for 40 cycles. The PCR system for miRNA used 25-μL reactions with the following conditions: 95 °C for 10 s; 95 °C for 5 s and 60 °C for 20 s for 40 cycles. The relative expression of mRNAs and miRNAs were calculated using the comparative $2^{-\Delta\Delta Ct}$ method (Cui et al., 2022) and normalized to *U6* and *β-actin*, respectively.

2.2.10 Statistical analysis

The difference of mean between the control and the treatment groups were analyzed using one-way ANOVA with Tukey's test adjustment. Pearson correlation coefficient of expression levels among novel-miR-144 and target genes were calculated. ANOVA and correlation analysis were performed using SPSS software (version 20.0, SPSS Inc., Chicago, IL, USA); $P<0.05$ was considered statistically significant. The statistical results were visualized by bar plots generated using ggplot2 (v3.3.5) package in R programming language (v4.1.0).

3 RESULT

3.1 Liver histology in response to heat stress

H&E staining showed the control group hepatic cells were arranged regularly with clear boundaries (Fig.1a). Under heat stress, liver tissues showed injuries that included edema, aggregation of blood cells, and slight damage with inflammatory cell infiltration, necrosis, and cells with displaced nuclei (Fig.1b). These histological results indicated that heat stress cause liver cell injury.

3.2 Pre-processing deep-sequencing data

For six paired-end mRNA libraries of largemouth bass livers, 21 795 175, 20 345 836, and 20 038 024 clean reads from the HT group, and 23 013 802, 23 846 026, and 21 857 888 clean reads from the CK group were obtained. The trimmed reads showed high quality (Table 1). After pre-processing of mRNA sequencing data, the derived transcriptome count matrix included total 106 171 404 read counts from 15 138 detected genes.

For six single-end miRNA libraries constructed using largemouth bass livers, the number of raw reads obtained from the six libraries were 17 492 392, 18 744 593, 18 005 520, 18 993 119, 18 492 171, and 17 717 699, respectively. After read trimming, 11 878 837 to 12 833 726 clean reads were obtained from each library (Table 2). Total 10 614 872 read counts from 925 conserved miRNAs and 140 predicted novel miRNAs were used to construct miRNA expression count matrix for the downstream analysis.

3.3 Differential gene expression analysis of DEGs and DEMs

Compared with the CK group, 406 DEGs were identified in the HT group, including 212 up-regulated mRNAs and 194 down-regulated mRNAs (Fig.2a; Supplementary Table S3). Totally, 47 miRNAs were significantly differentially expressed between

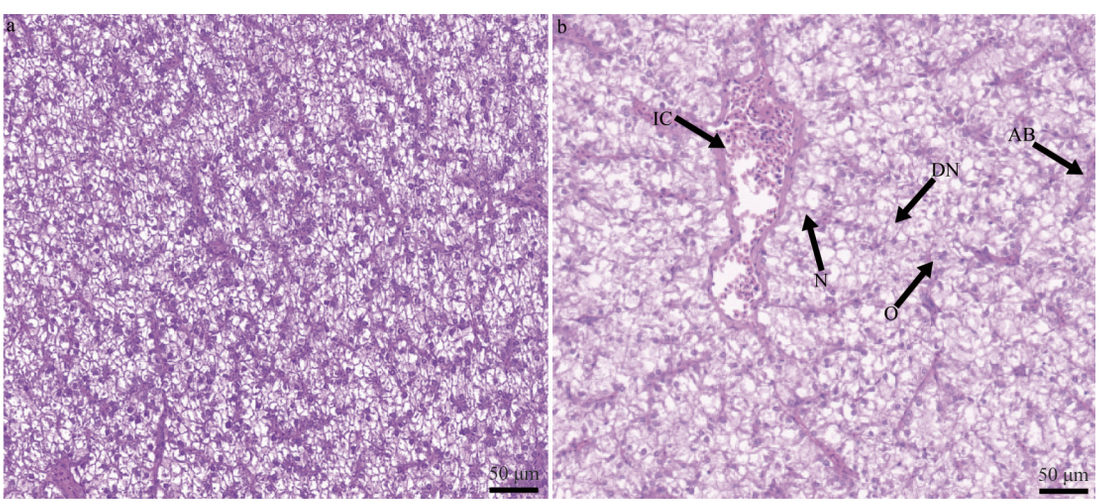

Fig.1 Photomicrographs of H&E-stained largemouth bass livers under control (a, 27 ℃) and heat stress condition (b, 37 ℃)

Heat stress group showed injuries that include oedema (O), aggregation of blood cell (AB), slight damage with inflammatory cell infiltration (IC), necrosis (N) and cells with displaced nuclei (DN). Scale bars=50 μm.

Table 1 Statistical evaluation of trimmed reads from mRNA sequencing

Sample ID	Read count	Base count	GC content (%)	Q20 (%)	Q30 (%)
CK1	23 013 802	6 893 845 612	49.32	97.67	93.63
CK2	23 846 026	7 144 535 682	49.05	97.44	93.18
CK3	21 857 888	6 543 319 078	49.49	97.74	93.71
HT1	21 795 175	6 530 135 154	49.45	97.53	93.20
HT2	20 345 836	6 088 134 882	49.30	97.26	92.61
HT3	20 038 024	5 996 796 968	49.44	97.68	93.58

Table 2 Statistical evaluation of trimmed reads from miRNA sequencing

Sample ID	Read count	Base count	GC content (%)	Q20 (%)	Q30 (%)
CK1	12 584 800	339 651 203	48.20	97.65	92.51
CK2	12 606 892	330 143 014	47.92	97.97	93.28
CK3	11 878 837	319 846 281	48.45	97.94	93.17
HT1	11 890 766	322 207 578	48.69	97.97	93.23
HT2	12 304 522	323 992 462	48.09	97.96	93.39
HT3	12 833 726	348 644 390	48.28	97.86	93.37

the CK and the HT groups (Fig.2b; Supplementary Table S4), 21 of which were up-regulated and 25 down-regulated. miR-375-3p, miR-375, miR-727-3p, miR-734-3p, and miR_135 were the most significantly up-regulated and miR-29b-2-5p, novel-miR-30, miR-206, miR-181a-3p, and novel-miR-3 were the most significantly down-regulated miRNAs (Supplementary Table S3).

3.4 Enrichment analysis of DEGs

Enriched GO terms and KEGG pathways of the identified DEGs were determined (Fig.3; Tables 3–4). In GO biological process terms, the most significantly enriched GO terms were related to macromolecule catabolic process (GO: 0009057), protein catabolic process (GO: 0030163), cellular macromolecule catabolic process (GO: 0044265), ornithine decarboxylase inhibitor activity (GO: 0008073), and cellular response to heat (GO: 0034605) (Fig.3a; Table 3). The most significantly enriched GO terms in cellular component classes were peptidase complex (GO: 1905368), proteasome regulatory particle (GO: 0005838), proteasome complex (GO: 0000502), endopeptidase complex (GO: 1905369), and proteasome accessory complex (GO: 0022624) (Fig.3a; Table 3). In GO molecular function items, DEGs were significantly enriched in unfolded protein binding (GO: 0051082), ornithine decarboxylase inhibitor activity (GO: 0008073), translation elongation factor activity (GO: 0003746), ornithine decarboxylase regulator activity (GO: 0042979), and ornithine decarboxylase activity (GO: 0004586) (Fig.3a; Table 3). KEGG enrichment analysis showed that most enriched DEGs were categorized as protein processing in endoplasmic reticulum (KEGG: 04141), steroid biosynthesis (KEGG: 00100), proteasome (KEGG: 03050), spliceosome (KEGG: 03040), and pyruvate metabolism (KEGG: 00620) (Fig.3b; Table 4).

3.5 The validation of the miRNA expression levels via qRT-PCR

The expression levels of selected DEMs were validated by qRT-PCR (Fig.4). The expressions of miR-375-3p, miR-727a-3p, miR-734-3p, novel-miR-135, and miR-181a-3p were up-regulated, while miR-181a-3p, miR-206, let-7b-3p, novel-miR-145, and novel-miR-30 expression showed a downward trend. The results of qRT-PCR are consistent with ones of miRNA-seq. Accordingly, these results support the reliability of our miRNA-seq data.

3.6 Integrated analysis of mRNAs and miRNAs

Target mRNAs were identified by intersecting the DEGs from RNA libraries with the miRNA target genes collected from miRanda and TargetScan. This analysis showed that 35 DEGs were predicted as target genes of 13 DEMs. The miRNA and mRNA interaction network showed that *cacnb4a*, *taf1*, *fryb*, and *rnf165b* might be negatively regulated by miR-222a-3p, while *zgc*: *91944* and *sqlea* might be positively regulated by miR-222a-3p. The *epb41l4b*,

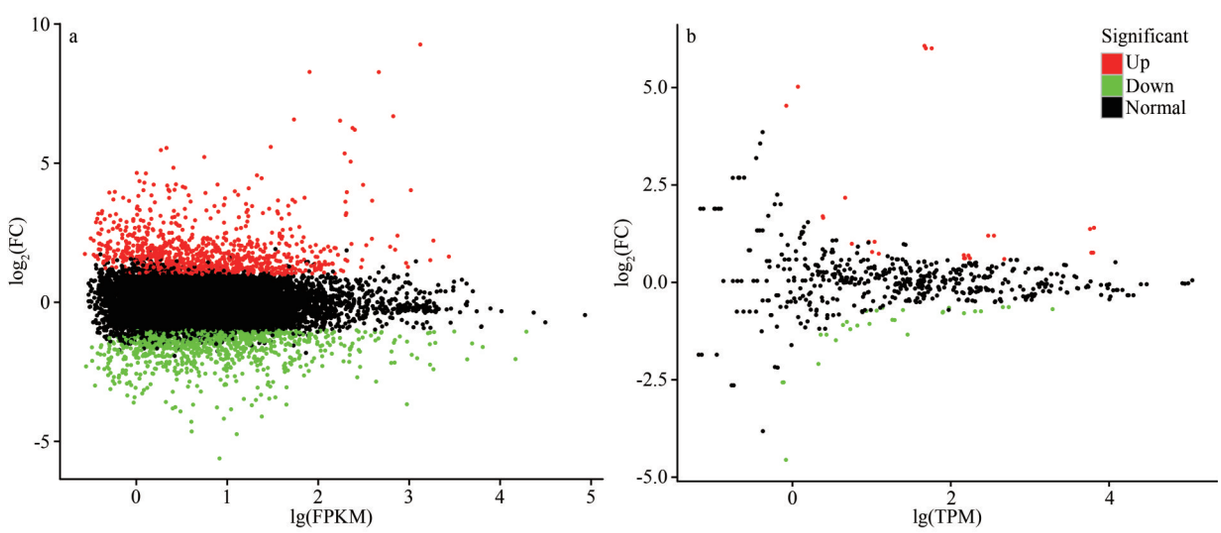

Fig.2 Mean-average (MA) plots of differential gene expression analysis between largemouth bass livers under control and heat stress condition based on mRNA (a) and miRNA data (b)

Significantly up and down regulated mRNAs/miRNAs were highlighted in red and green, respectively. FC: fold change; FPKM: fragments per kilo base of transcript per million mapped fragments; TPM: transcripts per million.

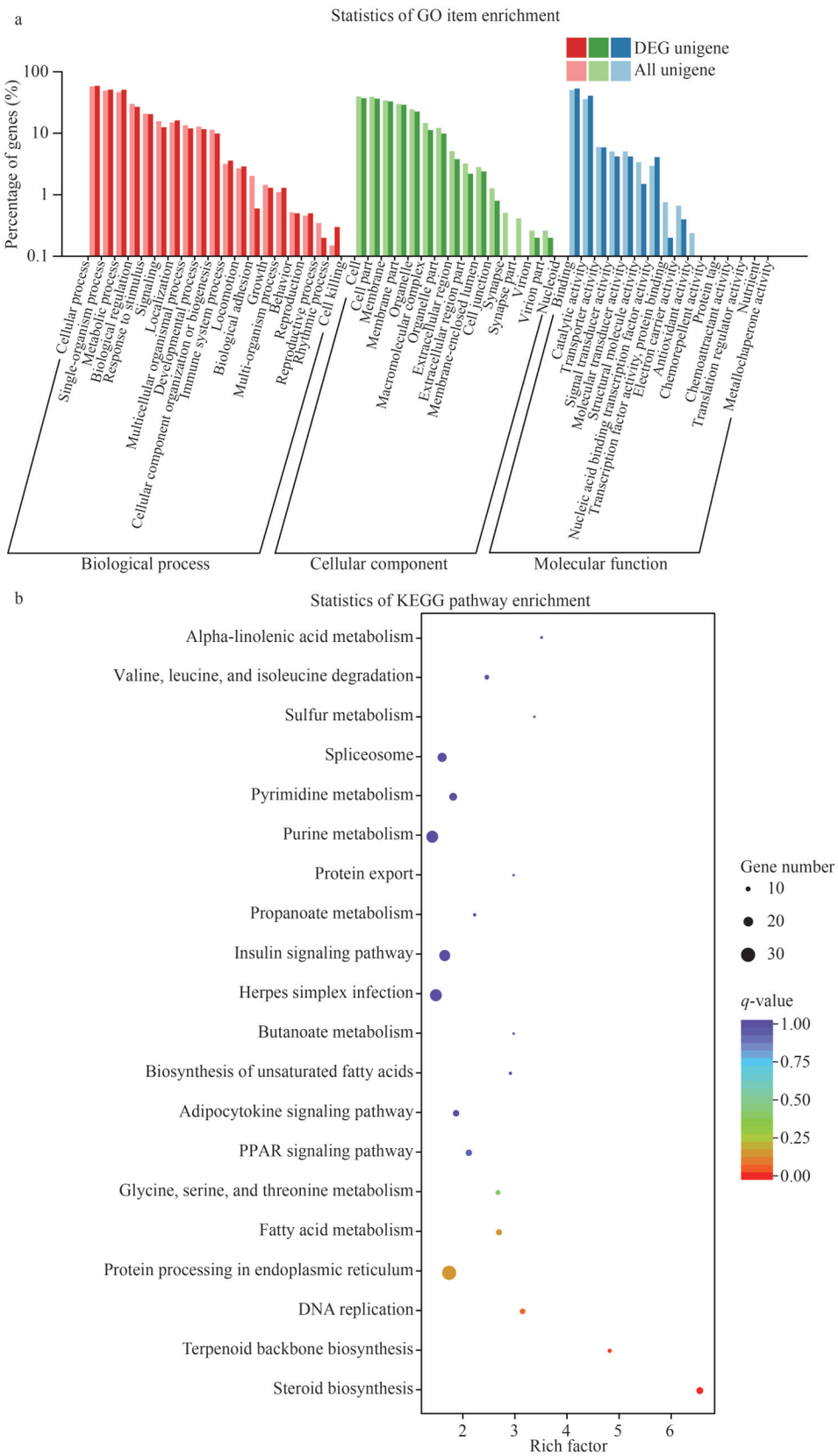

Fig.3 Functionally enriched GO terms (a) and KEGG pathways (b) analysis of DEGs in largemouth bass liver

Table 3 Significantly enriched Gene Ontology (GO) terms from enrichment analysis (adjusted *P*-value <0.05)

Category	ID	Description	Adj. *P*-value
BP	GO: 0009057	Macromolecule catabolic process	0.000
	GO: 0030163	Protein catabolic process	0.000
	GO: 0044265	Cellular macromolecule catabolic process	0.001
	GO: 0008073	Ornithine decarboxylase inhibitor activity	0.002
	GO: 0001878	Response to yeast	0.003
	GO: 0034605	Cellular response to heat	0.003
	GO: 0003746	Translation elongation factor activity	0.006
	GO: 0042176	Regulation of protein catabolic process	0.007
	GO: 0042979	Ornithine decarboxylase regulator activity	0.008
	GO: 0009620	Response to fungus	0.008
	GO: 0051603	Proteolysis involved in cellular protein catabolic process	0.013
	GO: 0006511	Ubiquitin-dependent protein catabolic process	0.013
	GO: 0044257	Cellular protein catabolic process	0.015
	GO: 0033157	Regulation of intracellular protein transport	0.018
	GO: 0019941	Modification-dependent protein catabolic process	0.018
	GO: 0006596	Polyamine biosynthetic process	0.020
	GO: 0043632	Modification-dependent macromolecule catabolic process	0.022
	GO: 0016126	Sterol biosynthetic process	0.023
	GO: 0009408	Response to heat	0.023
	GO: 0006595	Polyamine metabolic process	0.026
	GO: 0009266	Response to temperature stimulus	0.029
	GO: 1903827	Regulation of cellular protein localization	0.033
	GO: 0006979	Response to oxidative stress	0.039
	GO: 0010498	Proteasomal protein catabolic process	0.040
	GO: 0016125	Sterol metabolic process	0.047
	GO: 0009894	Regulation of catabolic process	0.050
	GO: 0006414	Translational elongation	0.050
CC	GO: 1905368	Peptidase complex	0.000
	GO: 0005838	Proteasome regulatory particle	0.000
	GO: 0000502	Proteasome complex	0.000
	GO: 1905369	Endopeptidase complex	0.000
	GO: 0022624	Proteasome accessory complex	0.000
	GO: 0031597	Cytosolic proteasome complex	0.001
	GO: 0008540	Proteasome regulatory particle, base subcomplex	0.007
	GO: 0008023	Transcription elongation factor complex	0.019
	GO: 0016604	Nuclear body	0.040
	GO: 0005788	Endoplasmic reticulum lumen	0.043
MF	GO: 0051082	Unfolded protein binding	0.000
	GO: 0008073	Ornithine decarboxylase inhibitor activity	0.000
	GO: 0003746	Translation elongation factor activity	0.001
	GO: 0042979	Ornithine decarboxylase regulator activity	0.001
	GO: 0004586	Ornithine decarboxylase activity	0.002
	GO: 0050661	NADP binding	0.004
	GO: 0030145	Manganese ion binding	0.013
	GO: 0008135	Translation factor activity, RNA binding	0.013
	GO: 0016831	Carboxy-lyase activity	0.017
	GO: 0090079	Translation regulator activity, nucleic acid binding	0.019
	GO: 0051787	Misfolded protein binding	0.022
	GO: 0000287	Magnesium ion binding	0.028
	GO: 0031072	Heat shock protein binding	0.042

BP, CC, and MF represent cellular component, biological process, and molecular function, respectively. Adj. *P*-value is adjusted *P*-value using Bonferroni step-down method.

Table 4 Significantly enriched Kyoto Encyclopedia of Genes and Genomes (KEGG) pathways from enrichment analysis (adjusted *P*-value <0.05)

ID	Description	Adj. *P*-value
KEGG: 04141	Protein processing in endoplasmic reticulum	0.000
KEGG: 00100	Steroid biosynthesis	0.001
KEGG: 03050	Proteasome	0.003
KEGG: 03040	Spliceosome	0.034
KEGG: 00620	Pyruvate metabolism	0.038

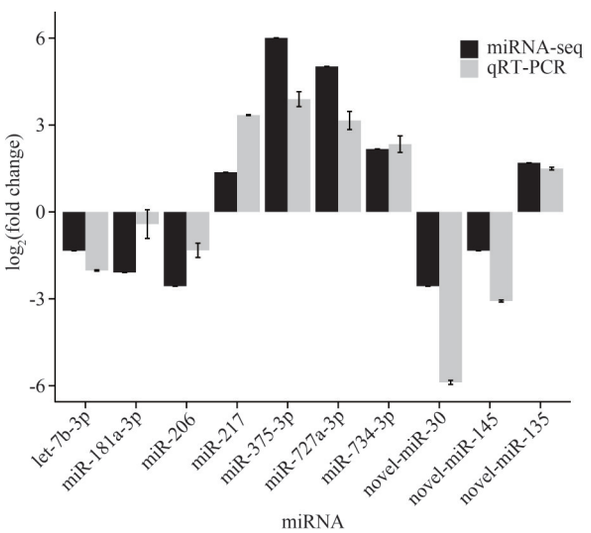

Fig.4 Validation of the miRNAs sequencing results using real-time PCR

xpo1b, *grb10b*, and *limk1a* might be negatively regulated by miR-30a-4-3p, while *wdr11* and *sema3aa* might be positively regulated by miR-30a-4-3p. The *ralgapa1* and *kdm2ab* might be negatively regulated by miR-125b-5p. *sesn2*, *loc116039764*, and *chd2 m*ight be positively regulated by miR-145-5p. *cep76*, *ankle2*, *loc116057223*, *plxnb1b*, *si*: *dkey*, *txndc5*, *acaca*, *atp10a*, and *cacna1c* might be negatively regulated by novel-miR-118, novel-miR-81, 29b-2-5p, miR-128-3p, miR-217, novel-miR-144, miR-375-3p, let-7j-5p, and novel-miR-63, respectively (Fig.5; Table 5).

3.7 Novel-miR-144 regulates apoptosis by targeting txndc5/ire1 signaling pathway

To determine a potential role of the novel-miR-144-txndc5/ire1 axis in heat stress, qPCR analysis was performed. The expression of novel-miR-144, *ire1*, *traf2*, *jnk1*, and *jnk2* were significantly up-regulated and the expression level of *txndc5* was significantly down-regulated under heat stress (Fig.6). In addition, the apoptosis-related genes (*caspase-3*, *caspase-8*, and *caspase-9*) were also significantly up-regulated in heat-stressed largemouth bass primary cells (Fig.6).

Pearson correlation analysis was performed to verify correlations between novel-miR-144 and the txndc5/ire1 axis. The expression of novel-miR-144 was strongly positively correlated with *grp94* expression (R=0.897, P<0.01). The expression of *txndc5* was significantly negatively correlated with *grp78* and *grp94* expression (R=-0.964, P<0.01 and R=-0.981, P<0.01, respectively). Thus, novel-miR-144 and *txndc5* may be involved in the regulation of ER homeostasis under heat stress. The expression of novel-miR-144 was significantly correlated with the expression of *txndc5*, *ire1*, *ask1*, *jnk1*, *jnk2*, and *caspase-9* (P<0.05). The expression of *txndc5* was significantly correlated with that of *ire1*, *traf2*, *ask1*, *jnk1*, *jnk2*, *caspase-3*, *caspase-8*, and *caspase-9* (P<0.01). novel-miR-144 may negatively regulate the *txndc5*/*ire1* axis and trigger apoptosis in the livers of largemouth bass under heat stress.

4 DISCUSSION

In the context of global warming, climate changes and extreme weather are becoming more frequent, which are expected to have inevitable effects on fish (Alfonso et al., 2021). In this study, our integrated miRNA and mRNA omics data revealed that novel-miR-144 negatively regulates *txndc5* and promotes apoptosis in the livers under heat stress. The results may enhance understanding of potential role of miRNAs that regulate fish under heat stress.

In this study, 406 DEGs were identified in the largemouth bass under heat stress, and these consisted of 212 up-regulated mRNAs and 194 down-regulated mRNAs. The “protein processing in endoplasmic reticulum” and “unfolded protein binding” pathways were significantly enriched in KEGG and GO analysis, respectively, which indicate the cellular response to the accumulation of abnormal proteins in the ER. Our findings are similar to the liver transcriptome results in pikeperch and rainbow trout under heat stress (Wang et al., 2019; Zhou et al., 2019), indicating that a large number of misfolded proteins accumulate in the ER of largemouth bass under heat stress. Accumulating misfolded proteins are usually transferred to the 26S proteasome for degradation; however, if the threshold volume that the proteasome can handle is exceeded, then the degradation

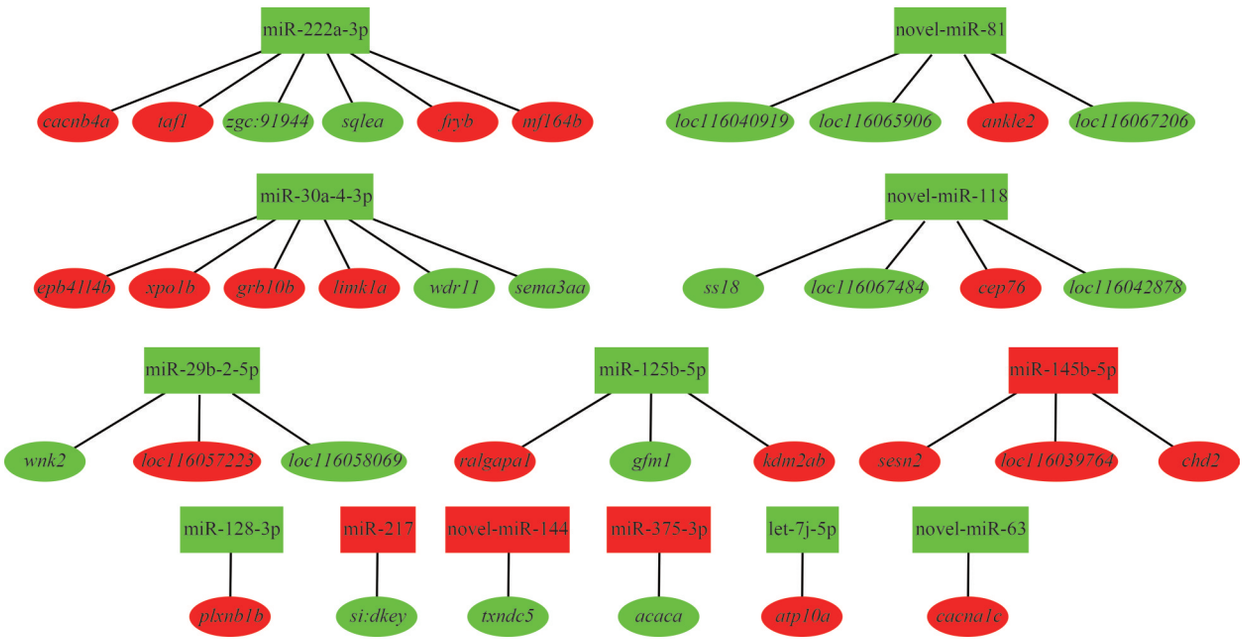

Fig.5 A network of miRNA-mRNA in largemouth bass liver under heat stress

Rectangles represent differentially expressed miRNAs and circles represent target differentially expressed genes. The red represents up-regulation, and the green represents down-regulation.

Table 5 Regulatory relationships between differentially expressed mRNAs and miRNAs

miRNA	Regulated	Target mRNA	Regulated
miR-222a-3p	Down	*zgc:91944*; *sqlea*	Down
miR-222a-3p	Down	*cacnb4a*; *taf1*; *fryb*; *rnf165b*	Up
miR-30a-4-3p	Down	*wdr11*; *sema3aa*	Down
miR-30a-4-3p	Down	*epb41l4b*; *xpo1b*; *grb10b*; *limk1a*	Up
novel-miR-81	Down	*loc116040919*; *loc116065906*; *loc116067206*	Down
novel-miR-81	Down	*ankle2*	Up
novel-miR-118	Down	*ss18*; *loc116067484*; *loc116042878*	Down
novel-miR-118	Down	*cep78*	Up
miR-29b-2-5p	Down	*wnk2*; *loc116058069*	Down
miR-29b-2-5p	Down	*loc116057223*	Up
miR-125b-5p	Down	*gfm1*	Down
miR-125b-5p	Down	*ralgapa1*; *kdm2ab*	Up
miR-145-5p	Up	*sesn2*; *loc116039764*; *chd2*	Up
miR-128-3p	Down	*plxnb1b*	Up
miR-217	Up	*si:dkey*	Down
novel-miR-144	Up	*txndc5*	Down
miR-375-3p	Up	*acaca*	Down
let-7j-5p	Down	*atp10a*	Up
novel-miR-63	Down	*cacna1c*	Up

machinery can be impaired and decreased (Karmon and Aroya, 2020). In this study, the "proteasome" was significantly enriched and the related genes (*psma2*, *psmc5*, *psmd1*, *psmd11b*, *psmd12*, *psmd2*, and *psme4a*), most of which belong to the 26s proteasome, were significantly down-regulated. We also found that "peptidase complex", "proteasome regulatory particle", "proteasome complex",

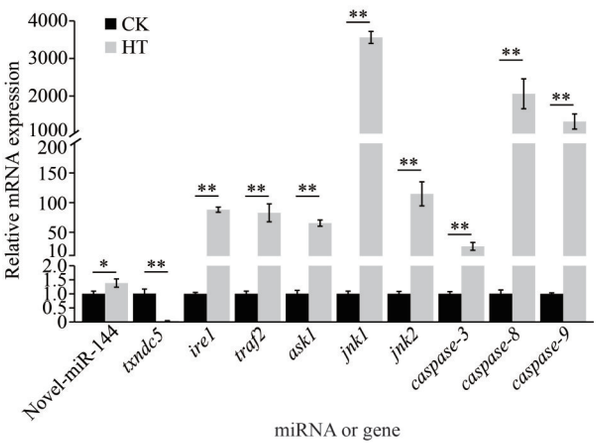

Fig.6 Relative expression of novel-miR-144 and genes related to endoplasmic reticulum stress under heat stress

*: $P<0.05$, **: $P<0.01$.

"endopeptidase complex", and "proteasome accessory complex" were also related to this process, indicating that protein degradation in largemouth bass may be blocked under heat stress. White and Wahl (2020) reported that the resting metabolic rates of largemouth bass inhabiting chronically heated lakes were significantly reduced. In our study, heat stress caused significant changes in the pathways of "ornithine decarboxylase inhibitor activity", "pyruvate metabolism", and "steroid biosynthesis". Ornithine, which is the hub of nitrogen metabolism in higher vertebrates, produces polyamines via ornithine decarboxylase, which activate protein translation (Zhang et al., 2020). When largemouth bass were subjected to heat stress, ornithine decarboxylase in the livers was suppressed, indicating that the translation of proteins may be reduced because of decreased ornithine metabolism, thereby relieving the protein burden. In our study, 10 DEGs were associated with the "pyruvate metabolism" and "steroid biosynthesis" pathways, including seven down-regulated genes related to lipid synthesis, i.e., *acaca*, *acat2*, *dhcr7*, *fdft1*, *msmo1*, *nsdhl*, and *sqlea*. The *me1* contributes to the cytoplasmic pool of nicotinamide adenine dinucleotide phosphate (NADPH), which is used by fatty acid synthase (Fernandes et al., 2018). In our study, the gene expression of *me1* was decreased, indicating that fatty acid synthesis was inhibited in largemouth bass under heat stress. The above results indicated that the accumulation of unfolded or misfolded proteins became a burden in largemouth bass, while inhibiting ornithine decarboxylase activity and decreasing lipid metabolism may be good mitigation strategies for largemouth bass in respond to heat stress. Heat shock proteins act as molecular chaperones that assist the folding and unfolding of proteins under certain adverse environmental stresses (Sita et al., 2017). Among the 15 hub genes, eight up-regulated genes, including *hsp90b1* (*grp94*), *hsp90aa1.1*, *hspa8* (*hsc70*), and *hspa5* (*grp78*), were significantly associated with "cellular response to heat" pathway, indicating that heat shock proteins may help largemouth bass restore protein homeostasis under heat stress.

miRNAs are post-transcriptional regulators of target mRNAs that induce RNA degradation, and many studies show that miRNAs are linked to various abiotic and biotic stresses (Dalmadi et al., 2019; Miao et al., 2022). In this study, we constructed an interaction network between DEMs and DEGs through integrated analyses. We found that miR-30a-4-3p could potentially target *xpo1b*, which transports heat stress factors from the nucleus to the cytoplasm in *Arabidopsis* under high irradiation (Huang et al., 2018). As a potential inhibitor of *xpo1b*, the expression level of miR-30a-4-3p was significantly down-regulated in largemouth bass livers under heat stress, indicating that it might be a regulator of heat stress factors in largemouth bass. RING finger protein 165 (Rnf165) is involved in E3 ubiquitin protein degradation (Kelly et al., 2013). In our study, miR-222a-3p was predicted to negatively regulate the expression of *rnf165*, indicating that miR-222a-3p might participate in the regulation of E3 ubiquitination in protein degradation in largemouth bass under heat stress. Partial loss of ANKLE2 disrupts the ER structure in *Drosophila* neuroblasts (Link et al., 2019). In our study, novel-miR-81 was predicted to negatively regulate the expression of *ankle2*, indicating that novel-miR-81 might be involved in protecting ER structures in largemouth bass. Recent evidence indicated that expression of miR-375 is associated with adipogenesis and apoptosis (Kraus et al., 2015; Wang et al., 2021). In this study, miR-375-3p inhibited the expression of *acaca*, similar to results from heat-stressed rainbow trout (Zhou et al., 2019). miR-375-3p may, therefore, be involved in lipid metabolism to relieve heat stress. Overall, based on the miRNA-mRNA interaction network, these DEMs may play vital roles in the response to heat stress by regulating their target genes.

Generally, apoptosis is a pathological response to liver injury (Bulanova et al., 2017; Wang et al., 2020; Cui et al., 2023), while the regulation of

miRNAs involved in apoptosis in fish under heat stress is poorly understood (Raza et al., 2022). The TATA-box binding protein associated factor 1 (TAF1) is vital during transcription initiation and is a regulator for apoptosis in response to genotoxic stress (Kimura et al., 2008). In our study, *taf1* was predicted to be negatively regulated by miR-222a-3p, indicating that miR-222a-3p might be a regulator of apoptosis in largemouth bass under heat stress. TXNDC5 is a member of the protein disulfide isomerase family that maintains proteostasis (Lee et al., 2020). Inhibiting the expression of TXNDC5 can induce ER stress-associated apoptosis in laryngeal squamous cell carcinoma cells (Peng et al., 2018). Here, we found that *txndc5* was significantly down-regulated in the largemouth bass livers under heat stress and significantly correlated with the expression of *caspase-3*, *caspase-8*, and *caspase-9*, indicating that *txndc5 m*ight be involved in largemouth bass liver apoptosis under heat stress. As a negative regulator of *txndc5*, the expression of novel-miR-144 was significantly increased in the present study and was correlated with the gene expression of *grp78*, *grp94*, and *caspase-9*, indicating that novel-miR-144 may be involved in ERS-induced apoptosis in largemouth bass under heat stress. Our previous study showed that IRE1/TRAF2/ASK1/JNK signaling mainly triggered apoptosis in largemouth bass livers under heat stress (Zhao et al., 2022). In the present study, the expression level of novel-miR-144 was consistent with that of IRE1 pathway genes, including *ire1*, *traf2*, *ask1*, and *jnk*. Moreover, it was significantly correlated with expression of *txndc5*, *ire1*, *ask1*, *jnk1*, *jnk2*, and *caspase-9* (P<0.05). Together, the above findings indicate that novel-miR-144 activated IRE1 signaling pathway by targeting *txndc5* to induce liver apoptosis in largemouth bass under heat stress.

5 CONCLUSION

As important factors in post-transcriptional gene expression, miRNAs in fish under heat stress are rarely reported, while our research was an attempt to screen for DEMs in largemouth bass in the context of global warming. Investigation of the expression profiles of mRNA and miRNA were used to construct a co-expression miRNA-mRNA regulatory network. Our findings showed that increasing levels of unfolded or misfolded protein may lead to a metabolic burden for largemouth bass under heat stress and inhibiting ornithine decarboxylase activity and decreasing lipid metabolism may be a good strategy for largemouth bass to resist heat stress. We also revealed that novel-miR-144 might negatively regulate *txndc5* and promote apoptosis in the livers of largemouth bass under heat stress. Overall, the findings of this study provided valuable information of the physiological alterations that largemouth bass undergo in response to global warming, and also provided new understanding of thermal resistance at molecular level.

6 DATA AVAILABILITY STATEMENT

The data were deposited in the NCBI under accession Nos. PRJNA725023 and PRJNA744168.

References

Alfonso S, Gesto M, Sadoul B. 2021. Temperature increase and its effects on fish stress physiology in the context of global warming. *Journal of Fish Biology*, **98**(6): 1496-1508, https://doi.org/10.1111/jfb.14599.

Ashburner M, Ball C A, Blake J A et al. 2000. Gene Ontology: tool for the unification of biology. *Nature Genetics*, **25**(1): 25-29, https://doi.org/10.1038/75556.

Bae M J, Murphy C A, García-Berthou E. 2018. Temperature and hydrologic alteration predict the spread of invasive Largemouth Bass (*Micropterus salmoides*). *Science of the Total Environment*, **639**: 58-66, https://doi.org/10.1016/j.scitotenv.2018.05.001.

Bairoch A, Apweiler R. 1997. The SWISS-PROT protein sequence data bank and its supplement TrEMBL. *Nucleic Acids Research*, **25**(1): 31-36, https://doi.org/10.1093/nar/25.1.31.

Bao W D, Kojima K K, Kohany O. 2015. Repbase Update, a database of repetitive elements in eukaryotic genomes. *Mobile DNA*, **6**: 11, https://doi.org/10.1186/s13100-015-0041-9.

Bindea G, Mlecnik B, Hackl H et al. 2009. ClueGO: a Cytoscape plug-in to decipher functionally grouped gene ontology and pathway annotation networks. *Bioinformatics*, **25**(8): 1091-1093, https://doi.org/10.1093/bioinformatics/btp101.

Bulanova D, Ianevski A, Bugai A et al. 2017. Antiviral properties of chemical inhibitors of cellular anti-apoptotic Bcl-2 proteins. *Viruses*, **9**(10): 271, https://doi.org/10.3390/v9100271.

Cai L S, Wang L, Song K et al. 2020. Evaluation of protein requirement of spotted seabass (*Lateolabrax maculatus*) under two temperatures, and the liver transcriptome response to thermal stress. *Aquaculture*, **516**: 734615, https://doi.org/10.1016/j.aquaculture.2019.734615.

Chan P P, Lowe T M. 2009. GtRNAdb: A database of transfer RNA genes detected in genomic sequence. *Nucleic Acids Research*, **37**(Database issue): D93-D97, https://doi.org/10.1093/nar/gkn787.

Chen J Q, Zhang S, Tong J Y et al. 2020. Whole

transcriptome-based miRNA-mRNA network analysis revealed the mechanism of inflammation-immunosuppressive damage caused by cadmium in common carp spleens. *Science of the Total Environment*, **717**: 137081, https://doi.org/10.1016/j.scitotenv.2020.137081.

Cheng C H, Guo Z X, Luo S W et al. 2018. Effects of high temperature on biochemical parameters, oxidative stress, DNA damage and apoptosis of pufferfish (*Takifugu obscurus*). *Ecotoxicology and Environmental Safety*, **150**: 190-198, https://doi.org/10.1016/j.ecoenv.2017.12.045.

Cui J W, Zhou Q, Yu M J et al. 2022. 4-tert-butylphenol triggers common carp hepatocytes ferroptosis via oxidative stress, iron overload, SLC7A11/GSH/GPX4 axis, and ATF4/HSPA5/GPX4 axis. *Ecotoxicology and Environmental Safety*, **242**: 113944, https://doi.org/10.1016/j.ecoenv.2022.113944.

Cui J W, Qiu M N, Liu Y H et al. 2023. Nano-selenium protects grass carp hepatocytes against 4-tert-butylphenol-induced mitochondrial apoptosis and necroptosis via suppressing ROS-PARP1 axis. *Fish & Shellfish Immunology*, **135**: 108682, https://doi.org/10.1016/j.fsi.2023.108682.

Dalmadi Á, Gyula P, Bálint J et al. 2019. AGO-unbound cytosolic pool of mature miRNAs in plant cells reveals a novel regulatory step at AGO1 loading. *Nucleic Acids Research*, **47**(18): 9803-9817, https://doi.org/10.1093/nar/gkz690.

Díaz F, Re A D, González R A et al. 2007. Temperature preference and oxygen consumption of the largemouth bass *Micropterus salmoides* (Lacépède) acclimated to different temperatures. *Aquaculture Research*, **38**(13): 1387-1394, https://doi.org/10.1111/j.1365-2109.2007.01817.x.

Enright A J, John B, Gaul U et al. 2003. MicroRNA targets in *Drosophila*. *Genome Biology*, **5**(1): R1, https://doi.org/10.1186/gb-2003-5-1-r1.

Fernandes L M, Al-Dwairi A, Simmen R C M et al. 2018. Malic Enzyme 1 (ME1) is pro-oncogenic in $Apc^{Min/+}$ mice. *Scientific Reports*, **8**(1): 14268, https://doi.org/10.1038/s41598-018-32532-w.

Friedländer M R, MacKowiak S D, Li N et al. 2012. MiRDeep2 accurately identifies known and hundreds of novel microRNA genes in seven animal clades. *Nucleic Acids Research*, **40**(1): 37-52, https://doi.org/10.1093/nar/gkr688.

Grabherr M G, Haas B J, Yassour M et al. 2011. Full-length transcriptome assembly from RNA-Seq data without a reference genome. *Nature Biotechnology*, **29**(7): 644-652, https://doi.org/10.1038/nbt.1883.

Huang H Y, Chang K Y, Wu S J. 2018. High irradiance sensitive phenotype of *Arabidopsis hit2*/*xpo1a* mutant is caused in part by nuclear confinement of AtHsfA4a. *Biologia Plantarum*, **62**(1): 69-79, https://doi.org/10.1007/s10535-017-0753-4.

Huang X L, Liu S, Chen X et al. 2021. Comparative pathological description of nocardiosis in largemouth bass (*Micropterus salmoides*) and other Perciformes. *Aquaculture*, **534**: 736193, https://doi.org/10.1016/j.aquaculture.2020.736193.

Johnson N C, Xie S P, Kosaka Y et al. 2018. Increasing occurrence of cold and warm extremes during the recent global warming slowdown. *Nature Communications*, **9**: 1724, https://doi.org/10.1038/s41467-018-04040-y.

Kalvari I, Nawrocki E P, Ontiveros-Palacios N et al. 2021. Rfam 14: Expanded coverage of metagenomic, viral and microRNA families. *Nucleic Acids Research*, **49**(D1): D192-D200, https://doi.org/10.1093/nar/gkaa1047.

Kanehisa M, Goto S, Furumichi M et al. 2010. KEGG for representation and analysis of molecular networks involving diseases and drugs. *Nucleic Acids Research*, **38**(Database issue): D355-D360, https://doi.org/10.1093/nar/gkp896.

Kao Y C, Rogers M W, Bunnell D B et al. 2020. Effects of climate and land-use changes on fish catches across lakes at a global scale. *Nature Communications*, **11**: 2526, https://doi.org/10.1038/s41467-020-14624-2.

Karmon O, Aroya S B. 2020. Spatial organization of proteasome aggregates in the regulation of proteasome homeostasis. *Frontiers in Molecular Biosciences*, **6**: 150, https://doi.org/10.3389/fmolb.2019.00150.

Kassahn K S, Crozier R H, Ward A C et al. 2007. From transcriptome to biological function: environmental stress in an ectothermic vertebrate, the coral reef fish *Pomacentrus moluccensis*. *BMC Genomics*, **8**: 358, https://doi.org/10.1186/1471-2164-8-358.

Kelly C E, Thymiakou E, Dixon J E et al. 2013. Rnf165/Ark2C enhances BMP-Smad signaling to mediate motor axon extension. *PLoS Biology*, **11**(4): e1001538, https://doi.org/10.1371/journal.pbio.1001538.

Kimura J, Nguyen S T, Liu H S et al. 2008. A functional genome-wide RNAi screen identifies TAF1 as a regulator for apoptosis in response to genotoxic stress. *Nucleic Acids Research*, **36**(16): 5250-5259, https://doi.org/10.1093/nar/gkn506.

Kraus M, Greither T, Wenzel C et al. 2015. Inhibition of adipogenic differentiation of human SGBS preadipocytes by androgen-regulated microRNA miR-375. *Molecular and Cellular Endocrinology*, **414**: 177-185, https://doi.org/10.1016/j.mce.2015.07.026.

Langmead B, Trapnell C, Pop M et al. 2009. Ultrafast and memory-efficient alignment of short DNA sequences to the human genome. *Genome Biology*, **10**(3): R25, https://doi.org/10.1186/gb-2009-10-3-r25.

Lee T H, Yeh C F, Lee Y T et al. 2020. Fibroblast-enriched endoplasmic reticulum protein TXNDC5 promotes pulmonary fibrosis by augmenting TGFβ signaling through TGFBR1 stabilization. *Nature Communications*, **11**(1): 4254, https://doi.org/10.1038/s41467-020-18047-x.

Li B, Dewey C N. 2011. RSEM: accurate transcript quantification from RNA-Seq data with or without a reference genome. *BMC Bioinformatics*, **12**: 323, https://doi.org/10.1186/1471-2105-12-323.

Link N, Chung H, Jolly A et al. 2019. Mutations in *ANKLE2*, a ZIKA virus target, disrupt an asymmetric cell division pathway in *Drosophila* neuroblasts to cause microcephaly. *Developmental Cell*, **51**(6): 713-729. e6, https://doi.org/10.1016/j.devcel.2019.10.009.

Love M I, Huber W, Anders S. 2014. Moderated estimation of fold change and dispersion for RNA-seq data with

DESeq2. *Genome Biology*, **15**(12): 550, https://doi.org/10.1186/s13059-014-0550-8.

McGeary S E, Lin K S, Shi C Y et al. 2019. The biochemical basis of microRNA targeting efficacy. *Science*, **366**(6472): eaav1741, https://doi.org/10.1126/science.aav1741.

Miao Z Y, Miao Z R, Teng X H et al. 2022. Melatonin alleviates lead-induced intestinal epithelial cell pyroptosis in the common carps (*Cyprinus carpio*) via miR-17-5p/TXNIP axis. *Fish and Shellfish Immunology*, **131**: 127-136, https://doi.org/10.1126/j.fsi.2022.09.071.

Mistry J, Chuguransky S, Williams L et al. 2021. Pfam: the protein family's database in 2021. *Nucleic Acids Research*, **49**(D1): D412-D419, https://doi.org/10.1093/nar/gkaa913.

Mori M A, Ludwig R G, Garcia-Martin R et al. 2019. Extracellular miRNAs: from biomarkers to mediators of physiology and disease. *Cell Metabolism*, **30**(4): 656-673, https://doi.org/10.1016/j.cmet.2019.07.011.

Narum S R, Campbell N R. 2015. Transcriptomic response to heat stress among ecologically divergent populations of redband trout. *BMC Genomics*, **16**: 103, https://doi.org/10.1186/s12864-015-1246-5.

NCBI Resource Coordinators. 2018. Database resources of the national center for biotechnology information. *Nucleic Acids Research*, **46**(D1): D8-D13, https://doi.org/10.1093/nar/gkx1095.

Newton J R, Zenger K R, Jerry D R. 2013. Next-generation transcriptome profiling reveals insights into genetic factors contributing to growth differences and temperature adaptation in Australian populations of barramundi (*Lates calcarifer*). *Marine Genomics*, **11**: 45-52, https://doi.org/10.1016/j.margen.2013.07.002.

Nguinkal J A, Brunner R M, Verleih M et al. 2019. The first highly contiguous genome assembly of pikeperch (*Sander lucioperca*), an emerging aquaculture species in Europe. *Genes*, **10**(9): 708, https://doi.org/10.3390/genes10090708.

Olusanya H O, van Zyll de Jong M. 2018. Assessing the vulnerability of freshwater fishes to climate change in Newfoundland and Labrador. *PLoS One*, **13**(12): e0208182, https://doi.org/10.1371/journal.pone.0208182.

Peng F S, Zhang H L, Du Y H et al. 2018. Cetuximab enhances cisplatin-induced endoplasmic reticulum stress-associated apoptosis in laryngeal squamous cell carcinoma cells by inhibiting expression of TXNDC5. *Molecular Medicine Reports*, **17**(3): 4767-4776, https://doi.org/10.3892/mmr.2018.8376.

Quast C, Pruesse E, Yilmaz P et al. 2013. The SILVA ribosomal RNA gene database project: improved data processing and web-based tools. *Nucleic Acids Research*, **41**(Database issue): D590-D596, https://doi.org/10.1093/nar/gks1219.

Raza S H A, Abdelnour S A, Alotaibi M A et al. 2022. MicroRNAs mediated environmental stress responses and toxicity signs in teleost fish species. *Aquaculture*, **546**: 737310, https://doi.org/10.1016/j.aquaculture.2021.737310.

Shannon P, Markiel A, Ozier O et al. 2003. Cytoscape: A software Environment for integrated models of biomolecular interaction networks. *Genome Research*, **13**(11): 2498-2504, https://doi.org/10.1101/gr.1239303.

Shi K P, Dong S L, Zhou Y G et al. 2019. RNA-seq reveals temporal differences in the transcriptome response to acute heat stress in the Atlantic salmon (*Salmo salar*). *Comparative Biochemistry and Physiology Part D*: *Genomics and Proteomics*, **30**: 169-178, https://doi.org/10.1016/j.cbd.2018.12.011.

Sita K, Sehgal A, Hanumantharao B et al. 2017. Food legumes and rising temperatures: effects, adaptive functional mechanisms specific to reproductive growth stage and strategies to improve heat tolerance. *Frontiers in Plant Science*, **8**: 1658, https://doi.org/10.3389/fpls.2017.01658.

Sun J L, Zhao L L, Wu H et al. 2019. Analysis of miRNA-seq in the liver of common carp (*Cyprinus carpio* L.) in response to different environmental temperatures. *Functional and Integrative Genomics*, **19**(2): 265-280, https://doi.org/10.1007/s10142-018-0643-7.

Sun J L, Zhao L L, He K et al. 2020. MiRNA-mRNA integration analysis reveals the regulatory roles of miRNAs in the metabolism of largemouth bass (*Micropterus salmoides*) livers during acute hypoxic stress. *Aquaculture*, **526**: 735362, https://doi.org/10.1016/J.AQUACULTURE.2020.735362.

Wang C, Zhou Y L, Zhu Q H et al. 2018. Effects of heat stress on the liver of the Chinese giant salamander *Andrias davidianus*: histopathological changes and expression characterization of Nrf2-mediated antioxidant pathway genes. *Journal of Thermal Biology*, **76**: 115-125, https://doi.org/10.1016/j.jtherbio.2018.07.016.

Wang H Y, Yuan J, Dang X Q et al. 2021. Mettl14-mediated m6A modification modulates neuron apoptosis during the repair of spinal cord injury by regulating the transformation from pri-mir-375 to miR-375. *Cell and Bioscience*, **11**(1): 52, https://doi.org/10.1186/s13578-020-00526-9.

Wang X Q, Gao Y Z, Li Y et al. 2020. Roseotoxin B alleviates cholestatic liver fibrosis through inhibiting PDGF-B/PDGFR- β pathway in hepatic stellate cells. *Cell Death and Disease*, **11**(6): 458, https://doi.org/10.1038/s41419-020-2575-0.

Wang Y F, Li C J, Pan C L et al. 2019. Alterations to transcriptomic profile, histopathology, and oxidative stress in liver of pikeperch (*Sander lucioperca*) under heat stress. *Fish and Shellfish Immunology*, **95**: 659-669, https://doi.org/10.1016/j.fsi.2019.11.014.

White D P, Wahl D H. 2020. Growth and physiological responses in largemouth bass populations to environmental warming: effects of inhabiting chronically heated environments. *Journal of Thermal Biology*, **88**: 102467, https://doi.org/10.1016/j.jtherbio.2019.102467.

Woolway R I, Merchant C J. 2019. Worldwide alteration of lake mixing regimes in response to climate change. *Nature Geoscience*, **12**(4): 271-276, https://doi.org/10.1038/s41561-019-0322-x.

Xiang X J, Han S Z, Xu D et al. 2021. Effects of DGAT1 inhibition on hepatic lipid deposition, antioxidant capacity and inflammatory response in *Larimichthys*

crocea. *Aquaculture*, **543**: 736967, https://doi.org/10.1016/j.aquaculture.2021.736967.

Yu D, Zhang Z, Shen Z Y et al. 2018. Regional differences in thermal adaptation of a cold-water fish *Rhynchocypris oxycephalus* revealed by thermal tolerance and transcriptomic responses. *Scientific Reports*, **8**(1): 11703, https://doi.org/10.1038/s41598-018-30074-9.

Zhang J Y, Tao B H, Chong Y R et al. 2020. Ornithine and breast cancer: a matched case-control study. *Scientific Reports*, **10**(1): 15502, https://doi.org/10.1038/s41598-020-72699-9.

Zhao X Q, Li L L, Li C J et al. 2022. Heat stress-induced endoplasmic reticulum stress promotes liver apoptosis in largemouth bass (*Micropterus salmoides*). *Aquaculture*, **546**: 737401, https://doi.org/10.1016/j.aquaculture.2021.737401.

Zhou C Q, Zhou P, Ren Y L et al. 2019. Physiological response and miRNA-mRNA interaction analysis in the head kidney of rainbow trout exposed to acute heat stress. *Journal of Thermal Biology*, **83**: 134-141, https://doi.org/10.1016/J.JTHERBIO.2019.05.014.

Electronic supplementary material

Supplementary material (Supplementary Tables S1–S4) is available in the online version of this article at https://doi.org/10.1007/s00343-023-3003-y.